Journal of ELECTRICAL ENGINEERING, VOL 70 (2019), NO-7S, 101–106

sciendo

PAPERS

Preparation of rGO/Bi_2O_3 composites by hydrothermal synthesis for supercapacitor electrode

Wein-Duo Yang, Yu-Jiang Lin*

Reduced graphene oxide/bismuth oxide (rGO/Bi_2O_3) composites were prepared at various weight ratios of raw materials, GO and bismuth nitrate at 1:0.1, 1:0.3, 1:0.6, 1:0.9 and 1:1.2, respectively, by the improved Hummer's method. During the process, the mixed solutions were prepared, and then rGO was obtained by hydrothermal method. Finally, the complex of rGO/Bi_2O_3 was prepared by calcination after hydrothermal treatment. The results show that the removal of oxygen-containing functional groups in rGO are increased with the increase of graphene agglomeration, and the Raman shifts of G band tending to the lowest wave-number. The electrochemical characteristics of the as-prepared rGO/Bi_2O_3 materials were also examined in 1 M KOH electrolyte. The dominating charge storage mechanisms are attributed to the electric double layer behaviors. As the content of bismuth nitrate increased, the rGO/Bi_2O_3 had a higher capacitance. The rGO/Bi_2O_3 obtained from the weight ratio of GO and bismuth nitrate of 1:1.2 as raw materials exhibit a maximum specific capacitance of 216 Fg^{-1}, revealing that rGO/Bi_2O_3 obtained by hydrothermal synthesis method can be used for the carbon-electrode of a super capacitor.

K e y w o r d s: reduced graphene oxide, bismuth oxide, hydrothermal, capacitance

1 Introduction

Due to many advantages such as long cycle life, fast charging and high power density etc., supercapacitors attract attention for the new energy technology [1-3]. The specific capacitance of graphene ultracapacitor electrodes can reach 550 Fg^{-1}, which is relatively higher than those of the supercapacitors prepared by other carbon materials. Because of its unique structure and broad application prospects, it has been a research boom of graphene applied as an ultracapacitor electrode material [4].

Transition metal oxides such as NiO, RuO_2, MnO_2, Bi_2O_3, Co_3O_4, Fe_2O_3 and TiO_2 *etc* [5-7] exhibit high capacitance, but suffer from expensive price, low abundance and poor rate capability [8]. Typically, nanocrystalline Bi_2O_3 can offer a large surface area, electrochemical stability and pseudo capacitive behavior; it may make a significant contribution to the advancement of supercapacitor technology [9]. However, a disadvantage of the metal oxide material is its limited electric conductivity. Superior electrical conductivities and high specific area of graphene is a promising supercapacitor electrode material [10], therefore the combination of bismuth oxide and graphene may enhance the electrochemical properties of the overall system.

Yuan *et al* [11] indicated that nanosized Bi_2O_3 has been deposited on highly ordered mesoporous carbon via a simple deposition method. The specific capacitance of loaded Bi_2O_3 in the composite achieves 360 Fg^{-1} at 100 mVs^{-1}. Moreover, Xia *et al* [12] prepared worm–like mesoporous carbon@Bi_2O_3 composites electrode material, found excellent capacitance performance and the specific capacitance reached 386 Fg^{-1}, three times more than pure mesoporous carbon. Huang *et al* [13] prepared $Bi_2O_{2.33}$ microspheres for electrode material of supercapacitor. The $Bi_2O_{2.33}$ electrode reveals high specific capacitance (893 Fg^{-1} at 0.1 Ag^{-1}) with long cycle life. In 2014, Senthilkumar *et al* [14] assembled an asymmetric supercapacitor (ASC) using Bi_2O_3 as negative and activated carbon (AC) as positive electrodes with Li_2SO_4 as electrolyte. The specific capacitance can reach 99.5 Fg^{-1}.

In this work, we develop a hydrothermal method to synthesize the graphene nanosheet-bismuth oxide composite directly from graphite oxide (GO) and bismuth nitrate as the raw materials. Furthermore, various weight ratios of the raw materials were utilized to prepare rGO/Bi_2O_3 composites and materials properties were also characterized.

2 Experimental

2.1 Synthesis of rGO/Bi$_2$O$_3$

GO was prepared using the improved Hummer's method [15]. First, a strong acidic solution was obtained by mixing sulfuric acid and phosphoric acid. Natural graphite was added to the above mixture with vigorous agitation. Potassium permanganate ($KMnO_4$) was added

*Department of Chemical and Materials Engineering, National Kaohsiung University of Science and Technology, Kaohsiung 807, Taiwan, ywd@nkust.edu.tw

DOI: 10.2478/jee-2019–0049, Print (till 2015) ISSN 1335-3632, On-line ISSN 1339-309X

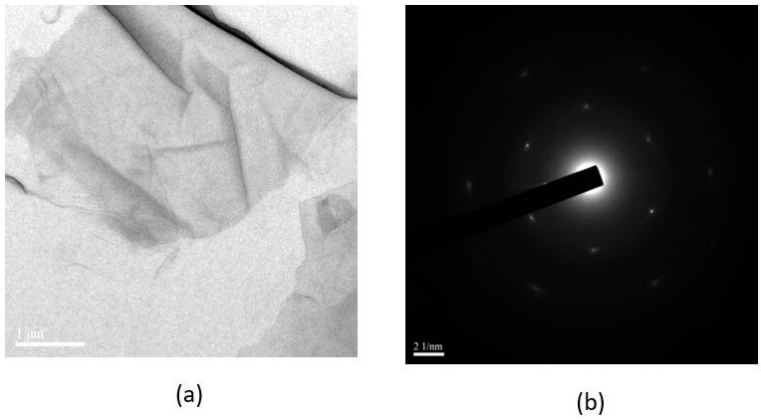

Fig. 1. (a) TEM image and (b) electron diffraction pattern of the as-prepared graphene oxide (GO)

slowly at 35 °C and reacted at stirring. Then, the reaction temperature was increased up to 50 °C and stirring at 600 rpm for 10 h until the mixture turned brownish. Finally, H_2O_2 was poured into the solution to terminate the oxidation of graphite. After centrifugation, acid washing, water washing, and vacuum drying, the brownish-yellow GO was prepared.

Various weight ratios of GO:$Bi(NO_3)_2$ $5H_2O$ raw materials were used to synthesize the as-prepared rGO/Bi_2O_3 composite materials by a hydrothermal method. Firstly, the as-synthesized GO was mixed with DI-water. A certain amount of $Bi(NO_3)_2$ $5H_2O$ was dissolved in nitric acid solution. And then, the above prepared solutions were mixed well. However, ammonium hydroxide was utilized to adjust the pH value at about 8.5. The mixed solution after ultra-sonicated and then put in an autoclave at 180 °C for 12 h. Finally, the resulting rGO/Bi_2O_3 obtained precursor was calcined in N_2 atmosphere. The weight ratios of GO:rGO/Bi_2O_3 were 1:0, 1:0.1, 1:0.3, 1:0.6, 1:0.9 and 1:1.2, respectively.

2.2 Characterization analyses and electrochemical properties

The physical properties of graphene oxide and the as-prepared reduced graphene oxide/Bi_2O_3 (rGO/Bi_2O_3) were investigated by transmission electron microscopy (TEM) (JEOL, TEM-3010) with an acceleration voltage of 80 kV, Raman spectroscopy (HORIBA, HR550) with a CCD detector (−70 °C), Fourier transform infrared spectroscopy (FTIR) (BIO, FIS-165) using the KBr pellet technique. Moreover, the surface area was determined by a Brunauer-Emmet-Teller (BET) analyzer (ASAP 2120; Micromeritics, Norcross, GA).

The mixture of rGO/Bi_2O_3, polytetrafluoroethylene as a binder, and black carbon as a conductive additive were dispersed in ethanol and then mixed to generate a homogeneous mixture. The resultant slurry was coated onto graphite paper as a current collector. The electrochemical properties were investigated using a conventional three-electrode cell system in 1 M KOH electrolyte by a cyclic voltammetry (CH Instruments, Model 400) method. The capacitance of the as-prepared material was obtained.

3 Results and discussion

Figure 1 shows the TEM image and electron diffraction pattern of the as-prepared graphene oxide (GO). It can be observed that the GO maintains the lamellar structure without aggregation and overlap, Fig. 1a. This is due to the incorporation of oxygen-containing functional groups, which can effectively impede the attraction of van der Waals force between graphene sheets. Thus, it can enable the observation of ruffling and curling of the sheets on the GO specimen. Figure 1b shows the electron diffraction patterns of the GO and reveals the typical graphene hexagonal ring-shaped electron diffraction spots [16]. It confirms that the experiment has successfully synthesized low layers of graphene oxide.

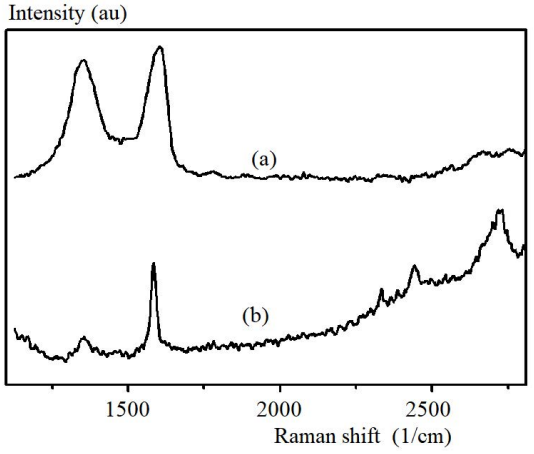

Fig. 2. The Raman spectra of (a) natural graphite sheets and (b) the as-prepared GO

Figure 2 shows the Raman spectra of natural graphite sheets and of the as-prepared GO. A weak peak near 1350 cm^{-1} (D band) of natural graphite sheet can be observed from Fig. 2a. The appearance of this peak corresponds to the natural defects of graphite sheet [17]. The

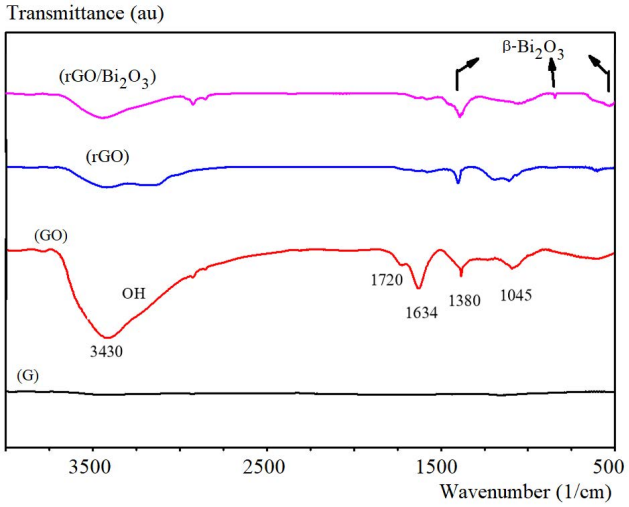

Fig. 3. FTIR spectra of graphite, GO, rGO and rGO/Bi2O3 samples

high intensity peak at near 1580 cm^{-1} (G band) corresponds to the characteristic peak of the sp^2 structure of the graphite sheet [18]. Furthermore, Fig. 2b shows the Raman spectrum of graphene oxide. The D band changes from the original weak peak to the high-intensity defect peak. It can be postulated that there are two reasons for this change. One is the oxidative environment caused by defects the combination of sulfuric acid and phospho-ric acid; and the other one is the impurities and defects caused by $KMnO_4$ strong oxidants at the preparatory process.

G band changed from a sharp peak into a widened sp^2 characteristic peak due to the strong oxidation reaction. The original graphite sheet of the regular stacking structure is affected by the formation of oxygen-containing functional groups by the strong oxidation, resulting in a decrease of GO symmetry and crystallization, which led to the appearance of broad peaks. The 2D band exhibits a faint peak shape relative to that of the natural graphite sheet, which means that the graphene prepared by the redox method is highly flawed and confused, leaving the photonic crystal lattice in which the 2D band cannot be in efficiently resonating.

Figure 3 shows FTIR spectra of graphite, GO, rGO and rGO/Bi_2O_3 samples. It shows that the natural graphite has no obvious absorption peak, Fig. 3a, due to the highly stable chemical nature. Compared with Fig. 3b, GO appeared an absorption peak at 3430 cm^{-1}, which is caused by the stretching vibration of –OH group. In addition, a broad band of absorption peaks appears in the range of 3000 – 3700 cm^{-1}, because the oxygen-containing functional groups introduced by oxidation of graphene oxide to facilitate water molecules to bond with GO layers by hydrogen bonding, and resulting in hydrophilic and water absorption [19]. The absorption peak near 1634 cm^{-1} corresponds to the bending vibration of the OH group. The absorption peak at 1720 cm^{-1} is the C=O stretching vibration of carbonyl group; the absorption peak at 1380 cm^{-1} is the stretching vibration of carboxyl CO group; the absorption peak near 1045 cm^{-1} caused by stretching vibration of C–OH. It can be demonstrated that graphene oxide is indeed rich in oxygen-containing functional groups through the action of strong oxidants, confirming the previous inference.

The FTIR spectra of rGO and rGO/Bi_2O_3 composites obtained by hydrothermally synthesized are shown in Fig. 3c and 3d, exhibiting the similar IR characteristics. Compared with GO, the –OH stretching vibration peak near 3430 cm^{-1} obviously weakened, while the absorption peak of oxygen-containing functional groups near 1634, 1720, 1380 and 1045 cm^{-1} also decreased, it reveals that hydrothermal synthesis of GO reduced to rGO, can indeed successfully to eliminate the oxygen-containing functional groups in the interlayer of rGO.

Figure 4 shows the adsorption-desorption curves of rGO and rGO/Bi_2O_3 samples. The as-prepared rGO/Bi_2O_3 was prepared from weight ratio of GO:bismuth nitrate at 1:1.2. Obviously, the isotherms exhibit typical type pattern of hysteresis loop and with no indication of a plateau at high P/P°, representing the characteristic of mesoporous material according to the classification of IUPAC. As seen from Fig. 4a, the relative pressure increases ($P/P^\circ > 0.85$), the adsorption isotherm rises sharply, indicating that N_2 has capillary condensation in the mesoporous material, and the amount of N_2-adsorption increases rapidly. Because the rGO material has a large pore size and a relatively larger amount of N_2 adsorbed, resulting the condensation of N_2 in the pores easily. For the rGO/Bi_2O_3 sample obtained from the weight ratio of

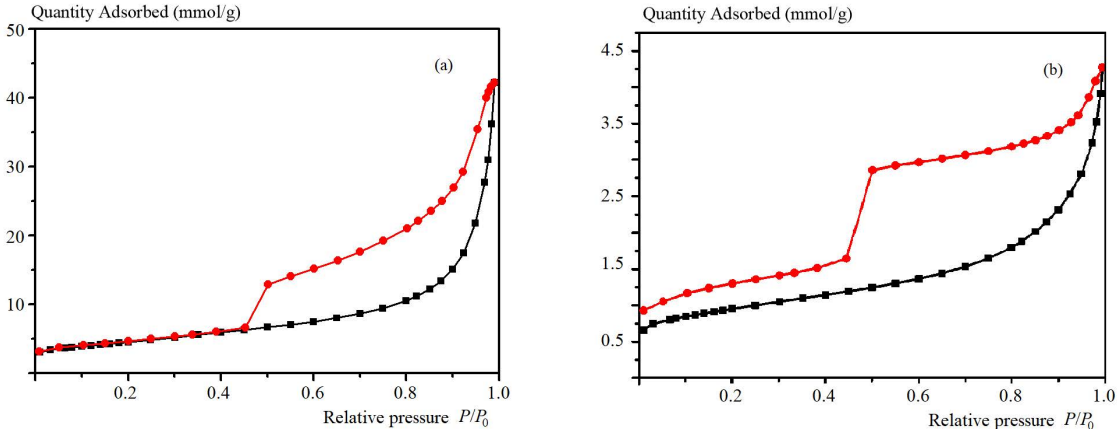

Fig. 4. Adsorption-desorption curves of (a) rGO and (b) rGO/Bi_2O_3 samples

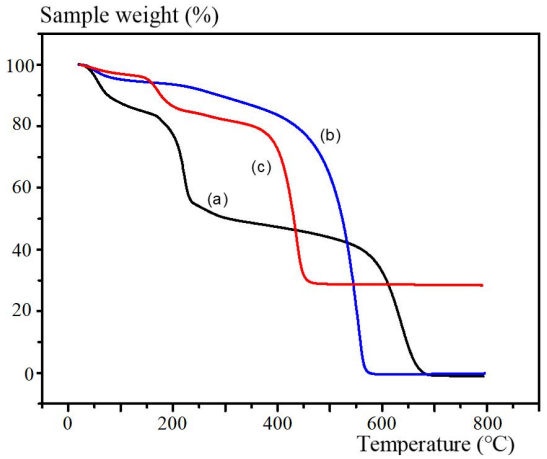

Fig. 5. The TGA analysis of GO, rGO and rGO/Bi_2O_3

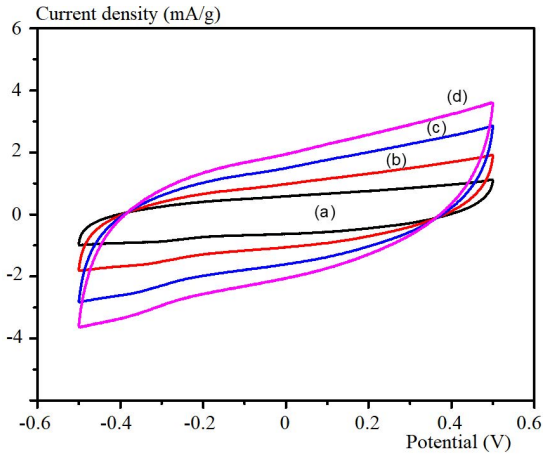

Fig. 6. The cyclic voltammograms of rGO at various scanning rates. (a) 10 mVs^{-1}, (b) 25 mVs^{-1}, (c) 50 mVs^{-1}, and (d) 75 mVs^{-1}.

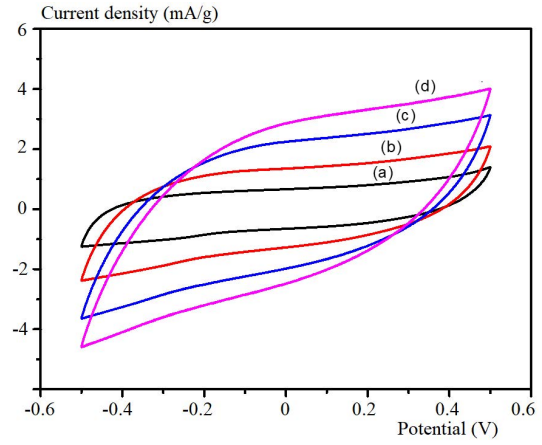

Fig. 7. The cyclic voltammograms of the as-prepared rGO/Bi_2O_3 at various scanning rates. (a) 10 mVs^{-1}, (b) 25 mVs^{-1}, (c) 50 mVs^{-1}, and (d) 75 mVs^{-1}.

GO: bismuth nitrate at 1:0.6, the hysteresis loops shifted to a lower adsorbed gas at any P/P° range, indicating that the pore size became smaller because the blockage of the rGO surface by Bi_2O_3 particles (Fig. 4b).

Table 1. The results obtained for specific surface area, pore volume, and average pore size from BET analysis

	SBET (m^2/g)	Pore Volume (cm^3/g)	Average pore size (nm)
rGO	358.9	1.46	16.28
rGO/Bi_2O_3	72.04	0.148	8.225

Table 1 shows the results obtained for specific surface area, pore volume, and average pore size from BET analysis. As seen from the table, it indicates that the as-prepared rGO possesses an average pore size of 16.28 nm with a specific surface area of 358.9 m^2g^{-1}. Whereas, the rGO/Bi_2O_3 obtained from the weight ratio of GO: bismuth nitrate at 1:0.6, with a specific surface area of 72.04 m^2g^{-1}, because the blockage of the rGO surface by Bi_2O_3 particles. In addition, the average pore diameter of the as-prepared rGO/Bi_2O_3 decreased to 8.225 nm, which was caused by the loading of Bi_2O_3 particles in the pores of graphene. Moreover, the original rGO had a pore volume of 1.46 cm^3g^{-1} and decreased to 0.148 cm^3g^{-1} after loading Bi_2O_3. It can be observed from the above results that rGO was indeed loaded with Bi_2O_3 nanoparticles, and the preparation of rGO/Bi_2O_3 composites was successful.

Hu *et al* [20] and Gao *et al* [21] reported rGO prepared by using the organic solvent reduction method. The specific surface area of the as-prepared rGO was 294.0 and 206.2 m^2g^{-1}, respectively. However, the specific surface area of reduced graphene oxide of this study is much higher than those scholars reported.

Figure 5 shows the TGA analysis of GO, rGO and rGO/Bi_2O_3. In Fig. 5a, there are a few weight losses near 100 °C, mainly due to the removal of moisture in the interlayer adsorption of graphene oxide. The weight loss is approximately 15%. Furthermore, the weight loss occurring near 200 °C is attributed to the removal of oxygen-containing functional groups in GO by the heat treatment [22]. In addition, during the TGA analysis, the graphene oxide undergoes a thermal reduction as the temperature increase, and the increase in graphene is agglomerated into a graphite form, which results in an increase in the decomposition temperature of the carbon component to approximately 590 °C. Figure 5b shows the TGA analysis of rGO. rGO mainly exhibits two decompositions: one occurs at approximately 100 °C as moisture is removed, while the other occurs at approximately 490 °C, demonstrating the thermal decomposition of rGO. Compared to GO, the carbon decomposition temperature of rGO decreased, confirming that the hydrothermally synthesized rGO contains higher graphene content. Figure 5c shows the TGA analysis of the rGO/Bi_2O_3 composite obtained

Table 2. The capacitance and Raman spectra data of the as-prepared rGO/Bi_2O_3 materials

Weight ratio of GO to bismuth nitrate	1:0	1:0.1	1:0.3	1:0.6	1:0.9	1:1.2
Specific capacitance (F/g)	83.5	87.6	103.2	196.0	204.7	216.0
G band of Raman spectra (cm^{-1})	1584.5	1587.3	1589.0	1590.8	1589.2	1587.3
R-value (I_D/I_G)	0.940	0.990	0.998	1.002	1.009	1.027

from the weight ratio of GO to bismuth nitrate of 1:0.6. A minor thermal decomposition occurred in the vicinity of 160 °C, presumably due to the decomposition of ammonium nitrate, which is a byproduct of the preparation of rGO/Bi_2O_3. In rGO/Bi_2O_3 composite materials, the delamination of Bi_2O_3 particles from the rGO interlaminar structures resulted in a decrease in the agglomerated rGO into graphite. The as-prepared rGO/Bi_2O_3, with a higher fraction of layered graphene, demonstrates the lowest carbon decomposition temperature of 400 °C. The final product contains the remaining 28% of the original weight in the form of Bi_2O_3. Hence, from this evidence, these study methods synthesized rGO/Bi_2O_3 composite materials.

Figure 6 shows the cyclic voltammograms of rGO at various scanning rates. The cyclic voltammograms indicate that the electric double layer is mainly utilized as the energy storage mechanism. Moreover, when the scan rate is increased, it can also maintain certain curve stability. It can be known that a small part of the activated oxygen-containing functional group enhances the infiltration between the electrode and the electrolyte, thereby, improving the conductivity of the composited electrode. Figures 7 shows the cyclic voltammograms of the as-prepared rGO/Bi_2O_3 at various scanning rates. The as-prepared rGO/Bi_2O_3 was prepared from weight ratio of GO:bismuth nitrate at 1:1.2. The results show that with the increase of scan rates, the curve still retains a certain area of the rectangle, which means that the rGO/Bi_2O_3 composite prepared in this study is an electrode material mainly composed of electric double layers and quasi-capacitive. It demonstrated a capacitance of 216 Fg^{-1} at 1 Ag^{-1} in 1 M KOH electrolyte.

Raman spectroscopy is a powerful tool to identify graphene. From the change of D band and G band the properties and quality of graphene can be determined. The conductivity and charge storage capacity of graphene are characterized. Table 2 shows the capacitance and Raman spectra data of the as-prepared rGO/Bi_2O_3 materials.

The relative intensity ratio of the D-band to G-band, defined as $R = I_D / I_G$, represents the structural order of graphene. The R-value was proposed to be an indication of disorder in GO or rGO. The smaller the R value, the greater the regularity. The R value of rGO is 0.94, which shows a higher order and lower randomness compared with other preparatory conditions. The R-value is 0.99 when rGO/Bi_2O_3 prepared at weight ratio of GO and bismuth nitrate at 1:0.1, 0.998 at 1:0.3, 1.002 at 1:0.6, 1.009 at 1:0.9, and 1.027 at 1:1.2. Obviously, with the increasing amount of Bi_2O_3, the R-value increases, indicating the more conversion of GO into rGO. Moreover, GO exhibits a Raman shift of G band to a high wavenumber offset, demonstrating a thin-layer (low layer-number) structure of graphene; and the lowest R value representing an ordered arrangement of graphene structure. The G band appearing at 1584.5 cm^{-1} implies that the absence of stabilized factor in the as-prepared rGO structure, resulting the agglomeration of part of the sp^2 layer-structure after hydrothermal synthesis. In addition, it involves the decomposition and reconstruction of the atomic structures during the reduction process of GO, lead to increase the defects and reduce the regularity of rGO, causing the R-value increased. Thus, the specific capacitance of rGO is about 83.5 Fg^{-1}.

As seen from in Tab. 2, as the concentration of Bi_2O_3 increases, the value of R will also increase, presumably because some impurities and defects are introduced during the preparation of Bi_2O_3. Moreover, the loading of Bi_2O_3 particles leads to the disorder of graphene. On the other hand, since the displacement (shift) of the G band is very sensitive to the thickness of graphene, the relative graphene thickness can be inferred from the displacement of the G band [23]. The rGO/Bi_2O_3 obtained from the weight ratio of GO and bismuth nitrate of 1:0.6 exhibits the highest wave number of the G band, revealing that graphene has the best degree of exfoliation and conductivity at this concentration. However, it also found that the specific capacitance of the above sample is not the highest, but continues to increase with increasing concentration. The highest specific capacitance value appears at the rGO/Bi_2O_3 obtained from the weight ratio of GO and bismuth nitrate of 1:1.2, about 216 Fg^{-1}. It is inferred that graphene achieves the best charge storage capacity at the rGO/Bi_2O_3 composition. With the increase of the concentration, more capacitance of the rGO/Bi_2O_3 composite materials will be gradually supplied by the quasi-capacitance of Bi_2O_3.

4 Conclusion

The rGO/Bi_2O_3 nano-composites were successfully prepared by a hydrothermal reduction method. Various weight ratios of the raw materials were utilized to explore the physical characteristics of the as-prepared rGO/Bi_2O_3. It revealed that oxygen-containing functional groups were largely eliminated and the GO was

successfully reduced to rGO. Furthermore, the increase of Bi_2O_3 increased the reduction of graphene oxide, and more Bi_2O_3 is intercalated into the multi-layer graphene oxide, resulting in a wider spacing of well-spelled reduced graphene oxide. However, the rGO exhibits a typical hexagonal spots structure of graphene. As the weight ratio of the raw materials, GO:nitrate increased up to 1:1.2, the G band wave-number of rGO/Bi_2O_3 is the highest, and the stripping effect of graphene is the best, demonstrating a specific capacitance of 216 Fg^{-1} in 1 M KOH electrolyte.

Acknowledgements

The authors wish to thank the Ministry of Science and Technology of Taiwan for its financial support of this work.

References

[1] C. Peng, S. Zhang, D. Jewell and G. Z. Chen, "Carbon nanotube and conducting polymer composites for supercapacitors", *Progress in Natural Science*, vol. 18, pp. 777–788, 2008.

[2] V. Augustyn, P. Simon and B. Dunn, "Pseudocapacitive oxide materials for high–rate electrochemical energy storage", *Energy & Environmental Science*, vol. 7, pp. 1597–1614,2014.

[3] S. Dai, Z. Liu, B. Zhao, J. Zeng, H. Hu, Q. Zhang, D. Chen, C. Qu, D. Dang and M. Liu, "A high–performance supercapacitor electrode based on N–doped porous graphene", *Journal of Power Sources*, vol. 387, pp. 43–48, 2018.

[4] S. Sekhar, M. J. Kim, K. S Yeom, S. S. A. An, H. Ju and D. K. Yi, "Trends in analytical chemistry Raman spectrum of graphene with its versatile future perspectives", *Trends Anal. Chem.*, vol. 80, pp. 25–131, 2016.

[5] K. Semishchenko, V. Tolstoy and A. Lobinsky, "A novel oxidation–reduction route for layer–by–layer synthesis of TiO_2 nanolayers and investigation of its photocatalytical properties", *J. Nanomater.*, pp. 632068, 2014.

[6] L. B. Gulina and V. P. Tolstoy, "The synthesis by successive ionic layer deposition of $SnMo_{0.6}O_y\ nH_2O$ nanolayers on silica", *Thin Sol. Films*, vol. 440, pp. 74–77, 2003.

[7] X. Liu, H. Zhu and X. Yang, "An amperometric hydrogen peroxide chemical sensor based on graphene–Fe_3O_4 multilayer films modified ITO electrode", *Talanta*, vol. 87, pp. 243–248, 2011.

[8] S. X. Wang, C. C. Jin and W. J. Qian, "Bi_2O_3 with activated carbon composite as a supercapacitor electrode", *Journal of Alloys and Compounds*, vol. 615, pp. 12–17, 2014.

[9] T. P. Gujar, V. R. Shinde, C. D. Lokhande and S. H. Han, "Electrosynthesis of Bi_2O_3 thin films and their use in electrochemical supercapacitors", *J. Power Sources*, vol. 161, pp. 1479–1485, 2006.

[10] B. Zhao, D. Chen, X. Xiong, B. Song, R. Hu, Q. Zhang, B. H. Rainwater, G. H. Waller, D. Zhen, Y. Ding,Y. Chen,C. Qu, D. Dang, C.-P. Wong, M. Liu, "A high–energy, long cycle–life hybrid supercapacitor based on graphene composite electrodes", *Energy Storage Materials*, vol. 7, pp. 32–39, 2017.

[11] D. S. Yuan, J. H. Zeng, N. Kristian, Y. Wang and X. Wang, "Bi_2O_3 deposited on highly ordered mesoporous carbon for supercapacitors", *Electrochem. Commun.*, vol. 11, pp. 313–317, 2009.

[12] N. N. Xia, D. S. Yuan, T. X. Zhou, J. Chen, S. Mo and Y. Liu, "Microwave synthesis and electrochemical characterization of mesoporous carbon@Bi_2O_3 composites", *Mater. Res. Bull.*, vol. 46, pp. 687–691, 2011.

[13] X. Huang, J. Yan, F. Zeng, X. Yuan, W. Zou and D. Yuan, "Facile preparation of orange–like $Bi_2O_{2.33}$ microspheres for high performance supercapacitor application", *Mater. Lett.*, vol. 90, pp. 90–92, 2013.

[14] S. T. Senthilkumar, R. K. Selvan, M. Ulaganathan and J. S. Melo, "Fabrication of Bi_2O_3 ‖ AC asymmetric supercapacitor with redoxadditive aqueous electrolyte and its improved electrochemicalperformances", *Electrochimica Acta*, vol. 115, pp. 518–524, 2014.

[15] J. Chen, B. Yao, C. Li and G. Shi, "An improved Hummers method for eco–friendly synthesis of graphene oxide", *Carbon*, vol. 64, pp. 225–229, 2013.

[16] W.-D. Yang, Y.-R. Li, and Y.-C. Lee, "Synthesis of r-GO/TiO_2 composites via the UV–assisted photocatalytic reduction of graphene oxide", *Applied Surface Science*, vol. 380, pp. 249–256, 2016.

[17] R. Yadav and C. K. Dixit, "Synthesis, characterization and prospective applications of nitrogen–doped graphene: A short review", *Journal of Science: Advanced Materials and Devices*, vol. 2, pp. 141–149, 2017.

[18] M. Lei, N. L. Zhc, C. Xie and H. Tang, "A peculiar mechanism for the photocatalyticreduction of decabromodiphenyl ether over reduced graphene oxide TiO_2 photocatalyst", *Chem. Eng. J.*, vol. 241, pp. 207–215, 2014.

[19] J. Liu, H. Bai, Y. Wang, Z. Liu, X. Zhang and D. D. Sun, "Self–assembling TiO_2 nanorods on large graphene oxide sheets at a two–phase interface and their anti–recombination in photocatalytic applications", *Adv. Funct. Mater.*, vol. 20, pp. 4175 –4181, 2010.

[20] R. Hu, X. Xiao, S. Tu, X. Zuo, and J. Nan, "Synthesis of flower–like heterostructured β-Bi_2O_3/$Bi_2O_2CO_3$ microspheres using $Bi_2O_2CO_3$ self–sacrifice precursor and its visible–light –induced photocatalytic degradation of o–phenylphenol", *Appl. Catal. B Environ.*, vol. 163, pp. 510–519, 2015.

[21] Z. Gao, X. Liu, J. Chang, D. Wu, F. Xu, L. Zhang, W. Du, and K. Jiang, "Graphene incorporated, N doped activated carbon as catalytic electrode in redox active electrolyte mediated supercapacitor", *J. Power Sources*, vol. 337, pp. 25–35, 2016.

[22] B. Xu, H. Wang, Q. Zhu, N. Sun, B. Anasori, L. Hu, F. Wang, Y. Guan and Y. Gogotsi, "Reduced graphene oxide as a multi–functional conductive binder for supercapacitor electrodes", *Energy Storage Materials*, vol. 12, pp. 128–136, 2018.

[23] D. Graf, F Molitor, K Ensslin, C. Stampfer, A. Jungen, C, Hierold, "Raman imaging of graphene", *J. Power Sources*, vol. 143, pp. 44–46, 2007.

Received 19 March 2019